

Bayesian analysis of diffusion-driven multi-type epidemic models with application to COVID-19

Lampros Bouranis^{*,1}, Nikolaos Demiris¹,
Konstantinos Kalogeropoulos², Ioannis Ntzoufras¹

¹*Department of Statistics, Athens University of Economics and Business,
Athens, Greece*

²*Department of Statistics, The London School of Economics and Political
Science, London, United kingdom*

* bouranis@aueb.gr

Abstract

We consider a flexible Bayesian evidence synthesis approach to model the age-specific transmission dynamics of COVID-19 based on daily age-stratified mortality counts. The temporal evolution of transmission rates in populations containing multiple types of individual are reconstructed via an appropriate dimension-reduction formulation driven by independent diffusion processes assigned to the key epidemiological parameters. A suitably tailored Susceptible-Exposed-Infected-Removed (SEIR) compartmental model is used to capture the latent counts of infections and to account for fluctuations in transmission influenced by phenomena like public health interventions and changes in human behaviour. We analyze the outbreak of COVID-19 in Greece and Austria and validate the proposed model using the estimated counts of cumulative infections from a large-scale seroprevalence survey in England.

Keywords: Bayesian evidence synthesis; Brownian motion; COVID-19; Hamiltonian Monte Carlo; Population epidemic model; Time-varying parameters.

1 Introduction

The COVID-19 outbreak caused by the Severe acute respiratory syndrome coronavirus 2 (SARS-CoV-2), has led to developments in Bayesian infectious disease modeling, allowing modelers to assess the impact of mitigation strategies on transmission and quantify the burden of the pandemic (Flaxman et al., 2020; Monod et al., 2021). The highly transmissible nature of COVID-19 has proven to be a challenge for health systems worldwide; large-scale seroprevalence studies aiming to estimate the actual number of infections have found severe under-ascertainment (Ward et al., 2021), which has been varying in time and across countries. The level of under-ascertainment depends on the national testing and tracing policies, the testing capacities and the impact of false positives under different regimes. Especially at the early stages of the pandemic, those tested were typically more likely to have been hospitalised or were at higher risk of infection or death, leading to only a proportion of infections being detected and

reported (Li et al., 2020). Methods that rely on reported counts of infections are expected to yield biases in the inferred rates of transmission.

This work addresses the challenges of under-ascertainment of COVID-19 infections and the presence of heterogeneity in type, relevance, and granularity of the data. Following the approach by Flaxman et al. (2020) and its extension to multiple age groups by Monod et al. (2021), we propose a Bayesian evidence synthesis approach to model the age-stratified dynamics of COVID-19, with the aim to: (i) infer the true number of infections using age-stratified daily COVID-19 attributable mortality counts, which entail a higher degree of reliability compared to the daily number of reported infections; (ii) infer the age-stratified virus transmission rates from one group to another, with a particular focus on the transmission rate between and onto vulnerable groups which could support public health authorities in devising non-pharmaceutical interventions (NPIs) targeting these groups; (iii) reconstruct the age-stratified drivers of transmission during particular time periods and capture age-stratified trends in infections.

Chatzilena et al. (2022) assumed a homogeneously mixing population in which all individuals were equally susceptible and equally infectious should they become infected. The authors also assumed that the dynamic transmission rate between susceptible and infected individuals followed a stochastic process, see also Dureau et al. (2013). We extend this framework by developing an age-stratified transmission model with heterogeneous contact rates between age groups, which offers the advantages of relaxing the assumption of a homogeneous population, incorporates age structure and accounts for the presence of social structures. In particular, we target the transmission rate matrix process, the dimension of which increases quadratically with the number of age groups, and offer a dimension-reduction formulation projecting to latent diffusion processes. This formulation possesses several desirable characteristics in capturing the multiple group disease transmission mechanism: (i) it is based on a natural decomposition into the underlying biological and social components; (ii) it allows for further evidence synthesis utilising information from contact surveys; (iii) it is driven by a potentially non-scalar diffusion process to adequately capture the temporal evolution of the age-stratified transmission rates, as well as extrinsic environmental factors such as NPIs and climatic changes (Cazelles et al., 2021; Chatzilena et al., 2022; Gosh et al., 2022).

Our analysis integrates multiple data sources which are publicly available across countries: age-stratified daily COVID-19 attributable mortality counts, contact surveys, age-stratified daily laboratory-confirmed COVID-19 infection counts and the age distribution of the population. The contact survey data are used to delineate potential identifiability issues (Britton, 1998) at the unobserved infection rate level when those rates are decomposed in their social and biological component. In the following, the uncertainty in contact structure is expressed via suitable prior distributions.

The outline of the paper is as follows. Section 2 provides an overview of the multiple data sources and a presentation of the components of the Bayesian hierarchical model. In Section 3 we present the results of the empirical analysis for Greece and discuss the effect of model expansion on the inferred age-stratified transmission rates in order to resolve prior-data conflicts at a latent level. Results for Austria are presented in the Supplementary material. The proposed model is validated using estimations from a large-scale seroprevalence survey in England. We conclude the paper in Section 4 with final remarks.

2 Materials and Methods

2.1 Data sources

We modeled the dynamics of the SARS-CoV-2 epidemic in Greece, Austria and England. For each of these countries, we collected three types of data related to the SARS-CoV-2 epidemic: (i) the age distribution of reported deaths; (ii) the age distribution of all reported infections; (iii) the age distribution of the general population for each country, \mathbb{N} . The study period for Austria ranges from 2020-08-31 to 2021-03-28 (30 weeks). The study period for Greece ranges from 2020-09-01 to 2021-03-29 (30 weeks). For model validation, we analyse the period 2020-03-02 to 2021-09-27 (30 weeks) in England.

We adopted the country-specific synthetic contact matrices of Prem et al. (2021), which have been constructed upon adjusted contact patterns, based on national demographic and socioeconomic characteristics. In the absence of a synthetic contact matrix for England, we assumed that the respective synthetic contact matrix is represented by the synthetic contact matrix of Prem et al. (2021) for the United Kingdom. The elements of these matrices represent the daily average numbers of contacts between age groups.

The severity of the disease is incorporated in the model via the age-stratified infection fatality rate (IFR). The age-stratified IFR in our model is informed by the REal-time Assessment of Community Transmission-2 (REACT-2) national seroprevalence study of over 100,000 adults in England (Ward et al., 2021). Detailed references for each data source are presented in Section S1 of the Supplementary material.

2.2 Modeling framework

2.2.1 Evidence synthesis

The aforementioned data streams and expert knowledge were integrated into a coherent modeling framework via a Bayesian evidence synthesis approach (De Angelis and Presanis, 2018). The proposed framework offers the advantage of estimation of disease transmission and estimation of various hidden characteristics of the disease like the latent number of infections.

Following the works of Flaxman et al. (2020), Monod et al. (2021) and Chatzilena et al. (2022), the modeling process is separated into a latent epidemic process and an observation process in an effort to reduce sensitivity to observation noise and to allow for more flexibility in modeling different forms of data. Figure 1 shows the functional relationships between data sources, modeled outputs and parameters in this study. The components of the Bayesian hierarchical model are laid out in the remainder of Section 2.2.

2.2.2 Diffusion-driven multi-type transmission process

The transmission of COVID-19 is modeled through an age-stratified deterministic Susceptible-Exposed-Infectious-Removed (SEIR) compartmental model (Anderson and May, 1992) with Erlang-distributed latent and infectious periods. In particular, we introduce Erlang-distributed stage durations in the Exposed and Infected compartments and relax the mathematically convenient but unrealistic assumption of exponential stage durations (Anderson and Watson, 1980; Lloyd, 2001) by assuming that each of the Exposed and Infected compartments are defined by two stages, with the same rate of loss of latency (τ) and infectiousness (γ) in both stages. Removed individuals are assumed to be immune to reinfection for at least the duration of the study period.

The population is stratified into $\alpha \in \{1, \dots, A\}$ age groups and the total size of the age group is denoted by $N_\alpha = S_t^\alpha + E_{1,t}^\alpha + E_{2,t}^\alpha + I_{1,t}^\alpha + I_{2,t}^\alpha + R_t^\alpha$, where S_t^α represents the number of susceptible, $E_t^\alpha = \sum_{j=1}^2 E_{j,t}^\alpha$ represents the number of exposed but not yet infectious, $I_t^\alpha = \sum_{j=1}^2 I_{j,t}^\alpha$ is the number of infected and R_t^α is the number of removed individuals at time t at age group α . The number of individuals in each compartment is scaled by the total population $N = \sum_{\alpha=1}^A N_\alpha$, so that the sum of all compartments equals to one (Grinsztajn et al., 2021). The latent epidemic process is expressed by the following non-linear system of ordinary differential equations (ODEs) (Kermack and McKendrick, 1927)

$$\begin{cases} \frac{dS_t^\alpha}{dt} &= -\lambda_\alpha(t)S_t^\alpha, \\ \frac{dE_{1,t}^\alpha}{dt} &= \lambda_\alpha(t)S_t^\alpha - \tau E_{1,t}^\alpha, \\ \frac{dE_{2,t}^\alpha}{dt} &= \tau(E_{1,t}^\alpha - E_{2,t}^\alpha), \\ \frac{dI_{1,t}^\alpha}{dt} &= \tau E_{2,t}^\alpha - \gamma I_{1,t}^\alpha, \\ \frac{dI_{2,t}^\alpha}{dt} &= \gamma(I_{1,t}^\alpha - I_{2,t}^\alpha), \\ \frac{dR_t^\alpha}{dt} &= \gamma I_{2,t}^\alpha + \rho_\alpha \nu_{t-u}, \end{cases} \quad (1)$$

where the mean latent and infectious periods are $d_E = \frac{2}{\tau}$, $d_I = \frac{2}{\gamma}$, respectively. The number of new infections in age group α at day t is

$$\Delta_{t,\alpha}^{\text{infect}} = \int_{t-1}^t \tau E_{2,s}^\alpha ds. \quad (2)$$

The time-dependent force of infection $\lambda_\alpha(t)$ for age group $\alpha \in \{1, \dots, A\}$ is expressed as

$$\lambda_\alpha(t) = \sum_{\alpha'=1}^A \left[m_{\alpha,\alpha'}(t) \frac{(I_{1,t}^{\alpha'} + I_{2,t}^{\alpha'})}{N_{\alpha'}} \right],$$

which is a function of the proportion of infectious individuals in each age group $\alpha' \in \{1, \dots, A\}$, via the compartments $I_{1,t}^{\alpha'}$, $I_{2,t}^{\alpha'}$ divided by the total size of the age group $N_{\alpha'}$, and the time-varying person-to-person transmission rate from group α to group α' , $m_{\alpha,\alpha'}(t)$. We parameterize the transmission rate between different age groups $(\alpha, \alpha') \in \{1, \dots, A\}^2$ by

$$m_{\alpha,\alpha'}(t) = \beta_t^{\alpha\alpha'} \cdot C_{\alpha,\alpha'}, \quad (3)$$

breaking down the transmission rate matrix into its biological and social components (Baguelin et al., 2013; Knock et al., 2021): the social component is represented by the average number of contacts between individuals of age group α and age group α' via the contact matrix element $C_{\alpha,\alpha'}$; $\beta_t^{\alpha\alpha'}$ is the time-varying transmissibility of the virus, the probability that a contact between an infectious person in age group α and a susceptible person in age group α' leads to transmission at time t .

The formulation below may be viewed as a stochastic extension to the deterministic multi-type SEIR model, using diffusion processes for the coefficients $\beta_t^{\alpha\alpha'}$ in (3), driven by independent Brownian motions

$$\begin{cases} \beta_t^{\alpha\alpha'} &= \exp(x_t^{\alpha\alpha'}), \\ x_t^{\alpha\alpha'} \mid x_{t-1}^{\alpha\alpha'}, \sigma_x^{\alpha\alpha'} &\sim N(x_{t-1}^{\alpha\alpha'}, (\sigma_x^{\alpha\alpha'})^2), \\ dx_t^{\alpha\alpha'} &= \sigma_x^{\alpha\alpha'} dW_t^{\alpha\alpha'}, \\ dW_t^{\alpha\alpha'} &\sim N(0, dt), \end{cases} \quad (4)$$

with volatilities $\sigma_x^{\alpha\alpha'}$, corresponding to the case of little information on the shape of $\beta_t^{\alpha\alpha'}$. The volatility $\sigma_x^{\alpha\alpha'}$ plays the role of the regularizing factor: higher values of $\sigma_x^{\alpha\alpha'}$ lead to greater changes in $\beta_t^{\alpha\alpha'}$. The exponential transformation avoids negative values which have no biological meaning (Dureau et al., 2013; Cazelles et al., 2021). A major advantage of considering a diffusion process for modeling $\beta_t^{\alpha\alpha'}$ is its ability to capture and quantify the randomness of the underlying transmission dynamics, which is particularly useful when the dynamics are not completely understood. The diffusion process accounts for fluctuations in transmission that are influenced by non-modeled phenomena, such as new variants, mask-wearing propensity, etc. The diffusion process also allows for capturing the effect of unknown extrinsic factors on the age-stratified force of infection, for monitoring of the temporal evolution of the age-specific transmission rate without the implicit inclusion of external variables and for tackling non-stationarity in the data.

We propose a diffusion-driven multi-type latent transmission model which assigns independent Brownian motions to $\log(\beta_t^{11}), \log(\beta_t^{22}), \dots, \log(\beta_t^{AA})$ with respective age-stratified volatility parameters $\sigma_{x,\alpha}, \alpha \in \{1, \dots, A\}$, for reasons of parsimony and interpretability. The contact matrix is scaled by the age-stratified transmissibility in order to obtain the transmission rate matrix process

$$m_{\alpha,\alpha'}^{\text{MBM}}(t) = \beta_t^{\alpha\alpha'} \cdot C_{\alpha,\alpha'} \equiv \beta_t^{\alpha\alpha} \cdot C_{\alpha,\alpha'}, \quad (5)$$

under the assumption $\beta_t^{\alpha\alpha'} \equiv \beta_t^{\alpha\alpha}, \alpha \neq \alpha'$. Henceforth, we term the model in (5) by MBM (standing for Multi Brownian Motion). The MBM model can also be viewed as factor analysis, offering dimension reduction from all the elements of the transmission rate matrix process to the Brownian motions $\beta_t^{\alpha\alpha}$ for $\alpha \in \{1, \dots, A\}$. An appealing feature of this factor analysis representation is that it separates the contact matrix which reflects social components of the model and can be informed from survey data. We provide details on the formulation of the contact matrix in the Supplementary material.

Further reduction in the dimension of the transmission rate matrix process can be achieved by the formulation

$$m_{\alpha,\alpha'}^{\text{SBM}}(t) = \beta_t^{\alpha\alpha'} \cdot C_{\alpha,\alpha'} \equiv \beta_t \cdot C_{\alpha,\alpha'}, \quad (6)$$

under the assumption $\beta_t^{\alpha\alpha'} \equiv \beta_t$, where β_t is the time-varying transmissibility of the virus, the probability that a contact between an infectious person and a susceptible person leads to transmission at time t . Henceforth, we term the model in (6) by SBM (standing for Single Brownian Motion), which represents a nested model to MBM.

In related studies, Birrell et al. (2021) estimated the transmission rate between different age groups considering time-dependent (weekly-varying) contact matrices, not allowing the age-stratified transmissibility to vary unconstrained in time. Knock et al. (2021) considered a time-independent contact matrix; the transmission rate between different age groups was parameterised as in (6), however the virus transmissibility was assumed to be piecewise linear with multiple change points corresponding to major announcements and changes in COVID-19 related policy.

2.2.3 Observation process

Denote the number of observed deaths on day $t = 1, \dots, T$ in age group $\alpha \in \{1, \dots, A\}$ by $y_{t,\alpha}$. A given infection may lead to observation events (i.e deaths) in the future. A link between $y_{t,\alpha}$ and the expected number of new age-stratified infections is established via the function

$$d_{t,\alpha} = \mathbb{E}[y_{t,\alpha}] = \widehat{\text{IFR}}_{\alpha} \times \sum_{s=1}^{t-1} h_{t-s} \Delta_{s,\alpha}^{\text{infect}}$$

on the new expected age-stratified mortality counts, $d_{t,\alpha}$, the estimated age-stratified infection fatality rate, $\widehat{\text{IFR}}_\alpha$, and the infection-to-death distribution h , where h_s gives the probability the death occurs on the s^{th} day after infection, is assumed to be gamma distributed with mean 24.2 days and coefficient of variation 0.39 (Flaxman et al., 2020; Monod et al., 2021), that is

$$h \sim \text{Gamma}(6.29, 0.26). \quad (7)$$

We allow for over-dispersion in the observation processes to account for noise in the underlying data streams, for example due to day-of-week effects on data collection (Stoner et al., 2020; Knock et al., 2021), and link $d_{t,\alpha}$ to $y_{t,\alpha}$ through an over-dispersed count model (Hauser et al., 2020; Birrell et al., 2021; Seaman et al., 2022)

$$y_{t,\alpha} | \theta \sim \text{NegBin}(d_{t,\alpha}, \xi_{t,\alpha}), \quad (8)$$

where $\xi_{t,\alpha} = \frac{d_{t,\alpha}}{\phi}$, such that $\mathbb{V}[y_{t,\alpha}] = d_{t,\alpha}(1 + \phi)$. The log-likelihood of the observed deaths is given by

$$\ell^{\text{Deaths}}(y | \theta) = \sum_{t=1}^T \sum_{\alpha=1}^A \log \text{NegBin}(y_{t,\alpha} | d_{t,\alpha}, \xi_{t,\alpha}),$$

where $y \in \mathbb{R}_{0,+}^{T \times A}$ are the surveillance data on deaths for all time-points and age groups and the parameter vector corresponds to either θ^{SBM} or θ^{MBM} , defined in Section 2.3. The observation process in this work does not additionally model the age-stratified infection counts, for reasons discussed in Section 1.

2.3 Parameter estimation

Bayesian estimation of the parameters of the SBM and MBM models was performed using Markov chain Monte Carlo (MCMC). Computational details are provided in the Supplementary material. In the following we discuss the challenging aspects of parameter estimation and present inference approximations used in the implementation in order to improve mixing and computational efficiency.

Estimation of the new daily infection counts in (2) requires the solution of the non-linear system of ODEs in (1) coupled with the stochastic differential equation in (4), which together are cast as a hypo-elliptic diffusion which is intractable. We address the intractability of the hypo-elliptic diffusion by adopting the data augmentation framework of Dureau et al. (2013) as a means to infer the latent sample path x of the diffusion which is an infinite-dimensional object (Kalogeropoulos et al., 2010) and is indirectly observed through the time evolution of the disease states. The task of inference for the transmission rate(s) via diffusions is particularly challenging; modeling its time evolution at a more granular time-scale (i.e. at the time-points of the observations) would naturally increase the cost of the computational effort; to reduce the dimensionality of the stochastic process we split the study period into $k = 1, \dots, K$ weeks and denote by k_t the week that time point t falls into. We assumed that the transmissibility of the virus, β_{k_t} , remains constant between subsequent weeks $[k_t, k_t + 1)$ and employed time-discretization via an Euler-Maruyama approximation of the latent sample path x . Switching the notation from t to k_t , this implies $x_{k_t} | x_{k_t-1}, \sigma_x \sim \text{N}(x_{k_t-1}, \sigma_x^2)$ for the SBM model, which may be viewed as a prior distribution on x_{k_t} and decreases the dimensionality of the stochastic process to $K + 1 < T + 1$.

Another challenging aspect of parameter estimation is the estimation of the volatility σ_x which is a top-level parameter in the Bayesian hierarchical model; due to the multiple levels of

hierarchy in the evidence synthesis model (Figure 1) and the lack of information about it, this difficulty is reflected in the lower effective sample sizes in all of our analyses. Subsequently, this increases the difficulty to break down the transmission rate in (3) into its biological and social components. Finally, for this multivariate ODE time series model, the solution to (1) is approximated numerically via the Trapezoidal rule. Higher-order numerical ODE solvers can be considered, at the cost of increased computational effort.

The Bayesian hierarchical model is implemented via a dynamic Hamiltonian Monte Carlo algorithm (Betancourt, 2018) which utilizes gradient information to efficiently explore high-dimensional parameter spaces or complex posterior geometries and to obtain a sample from the posterior distribution of the model parameters given the observed data. The size of the parameter space increases with longer time horizons due to the involvement of the diffusion process in (4) at weekly level, making such a gradient-based MCMC method particularly suitable for the implementation of the Bayesian hierarchical model proposed in the work; simultaneously, this poses a challenge for ODE models, for which computing the gradient is computationally significantly more demanding and subtle than the plain likelihood evaluation (Timonen et al., 2022). The increasing computational cost as a consequence of increasing volumes of data for ODE models is a point raised by Birrell et al. (2021) and Gosh et al. (2022) and highlights the need for further developments in the area.

3 Application

3.1 The COVID-19 pandemic

The proposed methodology is illustrated on data from the COVID-19 pandemic in Greece between August 2020 and March 2021, where $K = 30$ weeks. The population was divided in three age groups, $\{0 - 39, 40 - 64, 65+\}$. During the study period, a national lockdown was implemented in November 2020 until the end of January, 2021. Some of the NPIs were relaxed at New Year’s Day (Table S3 of the Supplementary material). In this section we focus on the SBM model which accounts for the inherent variability of contacts in the population as a result of the response of individuals to NPIs which were taken to reduce transmission, expressing the uncertainty in contact structure via prior distributions on the elements of the random contact matrix C , which is constrained to not vary in time.

However, the assumption made in (6) restricts the age-stratified effective contact rates to be expressed by an overall effective contact rate for the population, which is dominated by the effective contact rate of the age group that drives the transmission of the virus, at the time-points of the observations (Figure 2, panel A). This non-realistic assumption does not properly account for the change in the behaviour of individuals at each age group over time as a result of the implementation of NPIs during the study period. As previously discussed in Section 2.3, the lack of sufficient information about the volatility σ_x increases the difficulty to break down the age-stratified transmission rate in (6) into its biological and social components, creating an identifiability issue. Therefore, any differences in the virus transmission procedure across strata are attributed to the random contact matrix elements $C_{\alpha,\alpha'}$, justifying the notable differences between the prior and the posterior distribution of the contact matrix (Figure 2, panel B). Consequently, the age-stratified transmission rate trajectories (Figure 2, panel C) only differ in terms of magnitude at the time-points of the observations.

The analysis of Austrian age-stratified mortality counts revealed the same view regarding the ability of the SBM model to capture the age-stratified trends in SARS-CoV-2 transmission (Figure S5 of the Supplementary material). These findings suggest that the SBM model is not

flexible enough to accommodate for age-stratified trends in SARS-CoV-2 transmission, motivating the need for a more flexible model which can better estimate the volatility of the diffusion process.

3.2 Model expansion

The assessment of the fidelity of the SBM model to the data at a latent level revealed an issue which may be seen as prior-data conflict at a latent level. We resolve this issue by expanding the SBM model to the MBM model in the spirit of Gustafson (2005) and inspecting the effect on the contact survey data.

The age-stratified mortality counts that are available from the national surveillance systems consistently indicate an increasing number of COVID-19 attributable deaths with age; for the case of Greece the respective time series for the younger age group, i.e. $\{0 - 39\}$, is sparsely-informed, while the elder age groups $\{40 - 64, 65+\}$ are well-informed; a similar observation can be made for the Austrian dataset (Figures S1-S4 of the Supplementary material). In the context of diffusion-driven transmission models it would be more sensible to group younger ages together so as to avoid sparsely-informed time series which are more difficult to fit and instead allow for more groupings in elder ages, i.e. by 5- or 10-year intervals, depending on the information that becomes available from the national surveillance systems. In such a case, where the number of age groups A is small, the mortality data do not provide much information on the top-level volatilities $\sigma_{x,\alpha}, \alpha \in \{1, \dots, A\}$ of the MBM Bayesian hierarchical model, reflecting the difficulty in the estimation of the volatility σ_x involved in the SBM model. Similarly to the SBM model, posterior inference of the age-stratified volatilities $\sigma_{x,\alpha}, \alpha \in \{1, \dots, A\}$ has resulted in lower effective sample sizes compared to the rest of the MBM model parameters.

The assumption of independent diffusions for the biological components of the age-stratified transmission rate in (5) allows for better reconstructing of the age-stratified drivers of transmission (Figure 3, panels A and C). The trajectory of the transmission rate of the age group $\{60+\}$ seems to be similar with the respective trajectory shown in Figure 2 Panel C, thus stressing the role of this group to the evolution of the epidemic. The rate of transmission reaches its highest point in October 2020 for all age groups; the largest magnitude is demonstrated for the age group $\{60+\}$ (Figure 3, panel C), providing evidence to support public health authorities in taking appropriate measures to decrease transmission within and between-groups. The order of magnitude of the age-stratified transmission rate changes between the SBM and MBM models because of the change in the order of magnitude in the posterior number of contacts (Figures 2 and 3, panel B). Overall, the expansion of the age-stratified transmission model offers better interpretability and more flexibility than the SBM model in inferring age-stratified dynamic transmission rates and enables the reconstruction of the age-stratified drivers of transmission. We discuss a quantitative comparison of the two models using information criteria in Section S2 of the Supplementary material.

The MBM model is validated in the period 2020-03-02 to 2021-09-27 ($K = 30$ weeks) using the estimated age-stratified numbers of cumulative infections in England from the REACT-2 seroprevalence survey (Ward et al., 2021). In the analysis the population was divided in three age groups, $\{0 - 39, 40 - 59, 60+\}$. REACT-2 quantified the total number of infected individuals in England and the level of under-ascertainment of infections in the population up to mid-July 2020; it was selected for model validation based on its careful design, large representative sample size and timing. The age-stratified estimated counts of cumulative infections from REACT-2 were adjusted by the age distribution of the population based on the three age groups $\{0 - 39, 40 - 59, 60+\}$. Figure 4 shows the agreement of the age-stratified model estimates

with the estimates from REACT-2 and demonstrates the ability of the MBM model to capture the level of under-ascertainment of infections over time and by age group.

4 Discussion

In this paper we have presented a novel approach to modeling the age-stratified dynamics of COVID-19 based on daily mortality counts. We proposed a flexible Bayesian evidence synthesis framework that avoids the need to make strict model assumptions about the age-specific transmission process and enables a data-driven modeling approach for inferring the mechanism governing COVID-19 transmission, based on diffusion processes that are a-priori independent. The modularity of the Bayesian approach allows for assessing fidelity to the data at a latent level and resolving the corresponding prior-data conflict via expanding the model to incorporate distinct diffusions for each age group.

There are several advantages associated with our approach. Our model is primarily driven by the reported daily COVID-19 attributable mortality counts; a key strength of our Bayesian evidence synthesis framework is that multiple data sources which are publicly available across countries are integrated to provide a robust overall picture of the epidemic nationwide: daily COVID-19 attributable mortality counts, daily laboratory-confirmed COVID-19 infection counts and the age distribution of the population. This increases the applicability of the model to multiple countries, since these data sources are made available by the national surveillance systems. A main contribution of this work is the data-driven estimation of the transmissibility of the virus via mutually independent diffusion processes, which remove the need for additional information regarding the timings of specific interventions and for hypotheses about their impact on transmission. Instead, more general assumptions need to be made, such as on the smoothness of the latent sample path of the age-stratified diffusion that we wish to infer.

Our approach allows policymakers to assess the effect of NPIs on each age group. The model simultaneously estimates multiple metrics of outbreak progression: by modeling mortality counts instead of inferring only from confirmed infections, the Bayesian hierarchical model is more robust to changes in COVID-19 testing policies and the ability of national healthcare systems to detect COVID-19 infections, i.e. through contact tracing, and provides valuable information about the age-stratified transmission rates, latent number of infections, reporting ratio and the effective reproduction number (Sections S4-S7 of the Supplementary material), where uncertainty is accounted for naturally via MCMC.

Our modeling approach is subject to limitations. Age-stratified counts of vaccinations are not accounted for in the latent transmission epidemic model in the form of covariates, but this does not pose an important limitation for the considered time period, with low counts of administered vaccinations until the end of March 2021. In its current form the proposed hierarchical model is suited for the pre-vaccine era. In addition, the model is limited by variations in the reporting procedure of deaths and mortality definitions across time and countries (Section S1 of the Supplementary material); the dates of daily reported deaths may deviate from the actual dates of deaths. The use of diffusion processes can be viewed as an attempt to model the noise within the observational model and mitigate such issues. Similar to the Bayesian models of Monod et al. (2021) and Wistuba et al. (2022), we make parametric assumptions regarding the distribution of the time between infection and reported death in (7) (i.e. it is assumed to be the same across age groups and constant during the study period). While factors like hospital capacity and vaccine efficacy are expected to affect the infection-to-death distribution, such parametric assumptions might not be generally transferable to countries with different reporting characteristics and healthcare systems.

Some further limitations are shared with the Bayesian model proposed in Knock et al. (2021). The latent transmission model assumes a closed environment, where no new infections are imported from outside of the population. Additionally, our model does not explicitly account for hospital-acquired infections which may have contributed to overall transmission and to persistence of infection in periods of high transmission. Age-specific counts of hospitalizations and intensive care unit cases (where publicly available) could help relax the parametric assumptions regarding the infection-to-death distribution and assist in the estimation of the course of the COVID-19 pandemic. The age-stratified IFR is crucial part of the observation model that enables estimation of the expected number of new infections from the observed mortality counts. An assumption that has been made is that the age-stratified IFRs remain constant during the study period. However, these are expected to vary in time and across populations due to a number of factors, such as SARS-CoV-2 variants, vaccine efficacy, the age distribution of the population, the age distribution of infections, underlying health conditions, access to healthcare resources, and other factors (Brazeau et al., 2022). Thus, dynamic age-stratified IFRs would be more appropriate when modeling the latent number of infections based on mortality data.

In future work we shall work on two directions to expand our model. The first will aim to incorporate dynamic age-stratified IFR estimates and integrate further healthcare surveillance data like age-stratified counts of vaccinations, hospitalizations and intensive care unit cases where these data are available. The second, motivated by multi-task Gaussian Processes which have been recently implemented for a different class of Bayesian infectious disease models (Seymour et al., 2022) could amend our model via exchangeable diffusion processes, reflecting a-priori beliefs that there is a shared structure between the dynamic transmission rates for individuals of different age groups.

Software

The **Bernadette** package for R (R Core Team, 2022) implements the methodology in this paper. The package, R code and documentation to reproduce the analysis are available at <https://github.com/bernadette-eu/indepgbm>.

Acknowledgments

The authors would like to thank Anastasia Chatzilena, Theodore Kypraios and David Rossell for their helpful and constructive comments. *Conflict of Interest*: None declared.

Funding

Lampros Bouranis' research is supported by the European Union's Horizon 2020 research and innovation programme under the Marie Skłodowska-Curie grant agreement No 101027218.

References

Anderson, D. and Watson, R. (1980). On the spread of a disease with gamma distributed latent and infectious periods. *Biometrika*, 67:191–198.

- Anderson, R. and May, R. (1992). *Infectious diseases of humans: dynamics and control*. Oxford university press, Oxford, United Kingdom.
- Baguelin, M., Flasche, S., Camacho, A., Demiris, N., Miller, E., and Edmunds, W. (2013). Assessing optimal target populations for influenza vaccination programmes: An evidence synthesis and modelling study. *PLoS Medicine*, 10(10):e1001527.
- Betancourt, M. (2018). A conceptual introduction to Hamiltonian Monte Carlo. <https://arxiv.org/abs/1701.02434>.
- Birrell, P., Blake, J., van Leeuwen, E., Gent, N., and De Angelis, D. (2021). Real-time now-casting and forecasting of COVID-19 dynamics in England: the first wave. *Phil. Trans. R. Soc. B*, 376:20200279.
- Brazeau, N., Verity, R., Jenks, S., Fu, H., Whittaker, C. and Winskill, P., Dorigatti, I., Walker, P., Riley, S., Schnekenberg, R., Hoeltgebaum, H., Mellan, T., Mishra, S., Unwin, H., Watson, O., Cucunuba, Z., Baguelin, M., Whittles, L., Bhatt, S., Ghani, A., Ferguson, N., and Okell, L. (2022). Estimating the COVID-19 infection fatality ratio accounting for seroreversion using statistical modelling. *Commun Med*, 2(54).
- Britton, T. (1998). Estimation in multitype epidemics. *J. R. Statist. Soc. B*, 60(4):663–679.
- Cazelles, B., Champagne, C., Nguyen-Van-Yen, B., Comiskey, C., Vergu, E., and Roche, B. (2021). A mechanistic and data-driven reconstruction of the time-varying reproduction number: Application to the covid-19 epidemic. *PLOS Computational Biology*, 17(7):1–20.
- Chatzilena, A., Demiris, N., and Kalogeropoulos, K. (2022). A modelling framework for the analysis of the transmission of SARS-CoV2. <https://arxiv.org/abs/2203.03773>.
- De Angelis, D. and Presanis, A. (2018). Analysing multiple epidemic data sources. In Held, L., Hens, N., O’Neill, P., and Wallinga, J., editors, *Handbook of Infectious Disease Data Analysis*. Chapman & Hall/CRC, Florida, USA.
- Dureau, J., Kalogeropoulos, K., and Baguelin, M. (2013). Capturing the time-varying drivers of an epidemic using stochastic dynamical systems. *Biostatistics*, 14(3):541–555.
- Flaxman, S., Mishra, S., Gandy, A., Unwin, H., Mellan, T., Coupland, H., Whittaker, C., Zhu, H., Berah, T., and Eaton, J. (2020). Estimating the effects of non-pharmaceutical interventions on COVID-19 in Europe. *Nature*, 584(7820):257–261.
- Gosh, S., Birrell, P., and De Angelis, D. (2022). An approximate diffusion process for environmental stochasticity in infectious disease transmission modelling. <https://arxiv.org/abs/2208.14363>.
- Grinsztajn, L., Semenova, E., Margossian, C., and Riou, J. (2021). Bayesian workflow for disease transmission modeling in stan. *Statistics in Medicine*, 40(27):6209–6234.
- Gustafson, P. (2005). On Model Expansion, Model Contraction, Identifiability and Prior Information: Two Illustrative Scenarios Involving Mismeasured Variables. *Statistical Science*, 20(2):111–140.
- Hauser, A., Counotte, M., Margossian, C., Konstantinoudis, G., Low, N., Althaus, C., and Riou, J. (2020). Estimation of SARS-CoV-2 mortality during the early stages of an epidemic: A modeling study in Hubei, China, and six regions in Europe. *PLOS Medicine*, 17(7):1–17.

- Kalogeropoulos, K., Roberts, G., and Dellaportas, P. (2010). Inference for stochastic volatility models using time change transformations. *The Annals of Statistics*, 38(2):784–807.
- Kermack, W. and McKendrick, A. (1927). A contribution to the mathematical theory of epidemics. *Proceedings of the Royal Society of London. Series A*, 115:700–721.
- Knock, E., Whittles, L., Lees, J., Perez-Guzman, P., Verity, R., FitzJohn, R., Gaythorpe, K., Imai, N., Hinsley, W., Okell, L., Rosello, A., Kantas, N., Walters, C., Bhatia, S., Watson, O., Whittaker, C., Cattarino, L., Boonyasiri, A., Djaafara, B., Fraser, K., Fu, H., Wang, H., Xi, X., Donnelly, C., Jauneikaite, E., Laydon, D., White, P., Ghani, A., Ferguson, N., Cori, A., and Baguelin, M. (2021). Key epidemiological drivers and impact of interventions in the 2020 SARS-CoV-2 epidemic in England. *Science Translational Medicine*, 13(602):eabg4262.
- Li, R., Pei, S., Chen, B., Song, Y., Zhang, T., Yang, W., and Shaman, J. (2020). Substantial undocumented infection facilitates the rapid dissemination of novel coronavirus (sars-cov-2). *Science*, 368(6490):89–493.
- Lloyd, A. (2001). Realistic distributions of infectious periods in epidemic models: Changing patterns of persistence and dynamics. *Theoretical Population Biology*, 60:59–71.
- Monod, M., Blenkinsop, A., Xi, X., Hebert, D., Bershan, S., Tietze, S., Bradley, V., Chen, Y., Coupland, H., Filippi, S., Ish-Horowicz, J., McManus, M., Mellan, T., Gandy, A., Hutchinson, M., Unwin, J., Vollmer, C., Michaela, A., Weber, S., Zhu, H., Bezancon, A., Ferguson, N., Mishra, S., Flaxman, S., Bhatt, S., and Ratmann, O. (2021). Age groups that sustain resurging COVID-19 epidemics in the United States. *Science*, 371(6536):eabe8372.
- Prem, K., Zandvoort, K., Klepac, P., Eggo, R., Davies, N., Cook, A., and Jit, M. (2021). Projecting contact matrices in 177 geographical regions: An update and comparison with empirical data for the COVID-19 era. *PLOS Computational Biology*, 17(7):1–19.
- R Core Team (2022). *R: A Language and Environment for Statistical Computing*. R Foundation for Statistical Computing, Vienna, Austria.
- Seaman, S., Samartsidis, P., Kall, M., and De Angelis, D. (2022). Nowcasting covid-19 deaths in england by age and region. *Journal of the Royal Statistical Society: Series C (Applied Statistics)*.
- Seymour, R., Kypraios, T., and O’Neill, P. (2022). Bayesian nonparametric inference for heterogeneously mixing infectious disease models. *Proceedings of the National Academy of Sciences*, 119(10):e2118425119.
- Stoner, O., Economou, T., and Halliday, A. (2020). A Powerful Modelling Framework for Nowcasting and Forecasting COVID-19 and Other Diseases. <https://arxiv.org/abs/1912.05965>.
- Timonen, J., Siccha, N., Bales, B., Lähdesmäki, H., and Aki Vehtari, A. (2022). An importance sampling approach for reliable and efficient inference in Bayesian ordinary differential equation models. <https://arxiv.org/abs/2205.09059>.
- Ward, H., Atchison, C., Whitaker, M., Ainslie, K., Elliott, J., Okell, L., Redd, R., Ashby, D., Donnelly, C., Barclay, W., Darzi, A., Cooke, G., Riley, S., and Elliott, P. (2021). Sars-cov-2 antibody prevalence in england following the first peak of the pandemic. *Nat Commun*, 12:905.

Wistuba, T., Mayr, A., and Staerk, C. (2022). Estimating the course of the COVID-19 pandemic in Germany via spline-based hierarchical modelling of death counts. *Scientific Reports*, 12(9784).

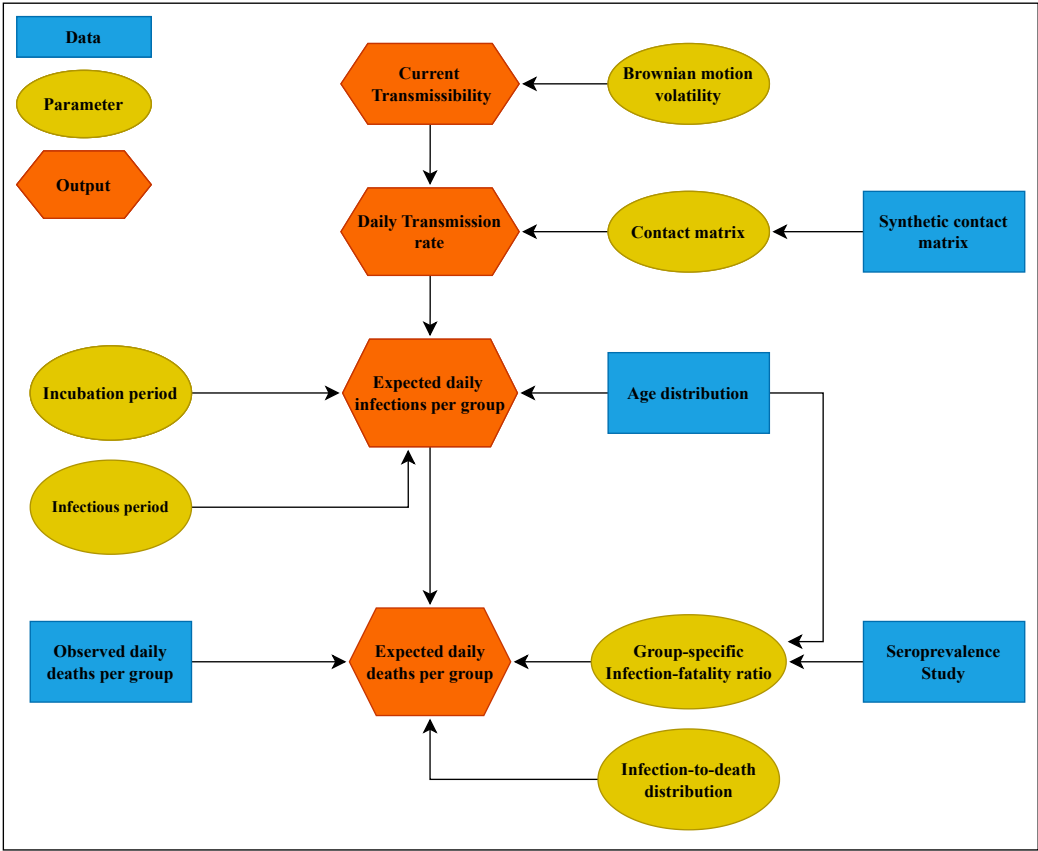


Figure 1: Functional relationships between data sources (rectangles), modeled outputs (ovals) and parameters (hexagons).

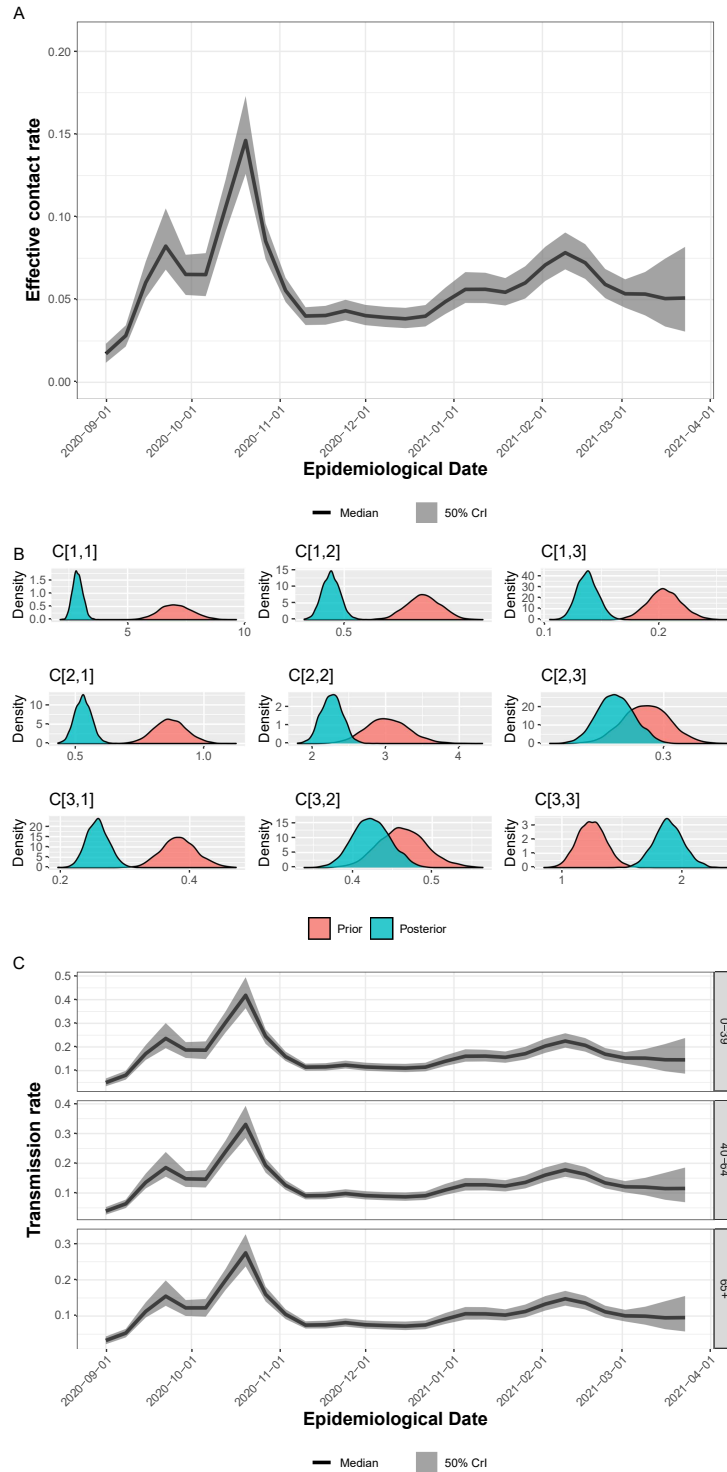


Figure 2: Greece - Components of the age-stratified transmission dynamics under the SBM transmission model. Estimated median posterior trajectory (50% credible interval, CrI) trajectory of the transmissibility of SARS-CoV-2 (panel A); prior and posterior distributions of each element of the contact matrix (panel B); estimated median posterior trajectory (50% credible interval, CrI) of the age-stratified transmission rate (panel C).

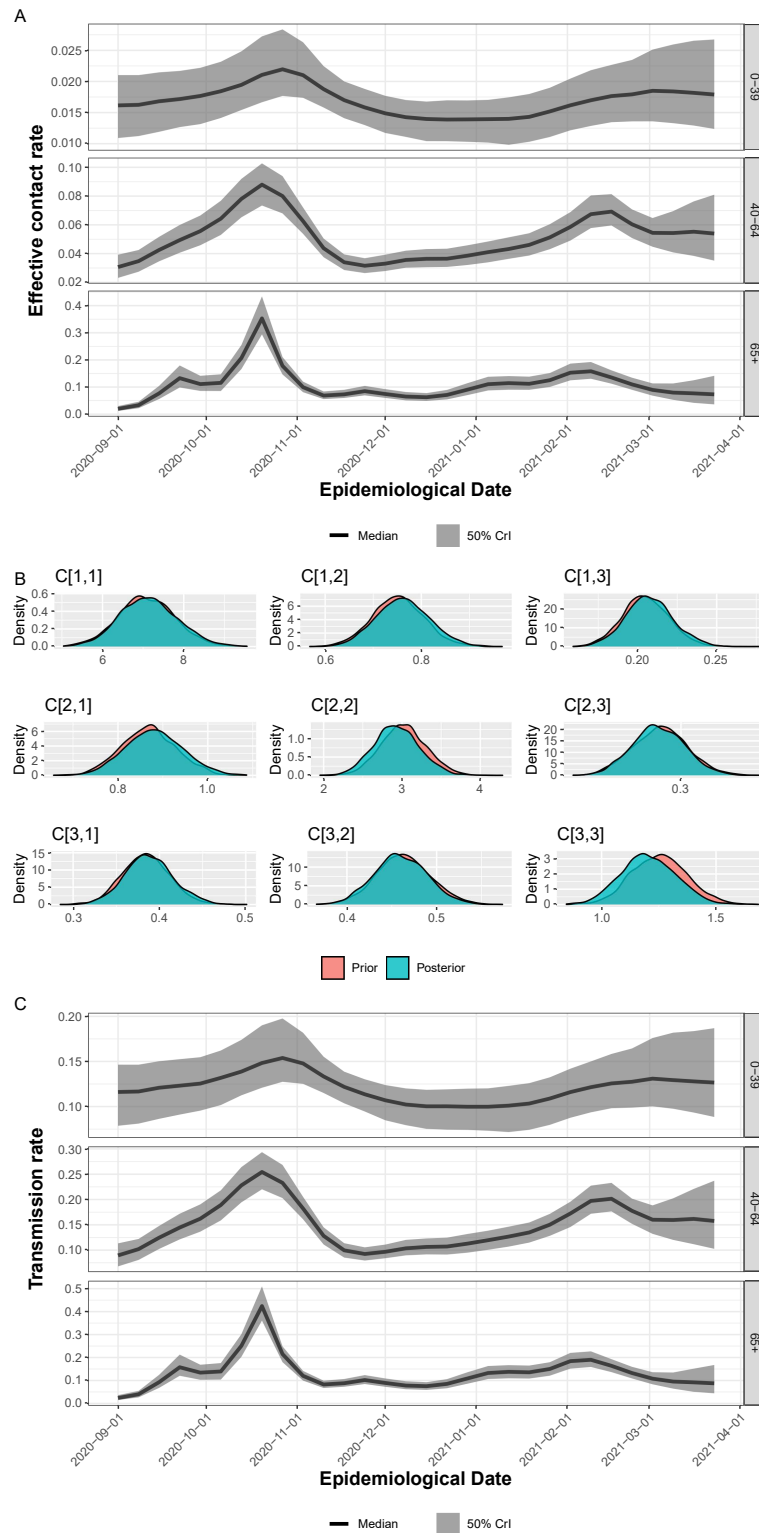


Figure 3: Greece - Components of the age-stratified transmission dynamics under the MBM transmission model. Estimated median posterior trajectory (50% credible interval, CrI) of the transmissibility of SARS-CoV-2 (panel A); prior and posterior distributions of each element of the contact matrix (panel B); estimated median posterior trajectory (50% credible interval, CrI) of the age-stratified transmission rate (panel C).

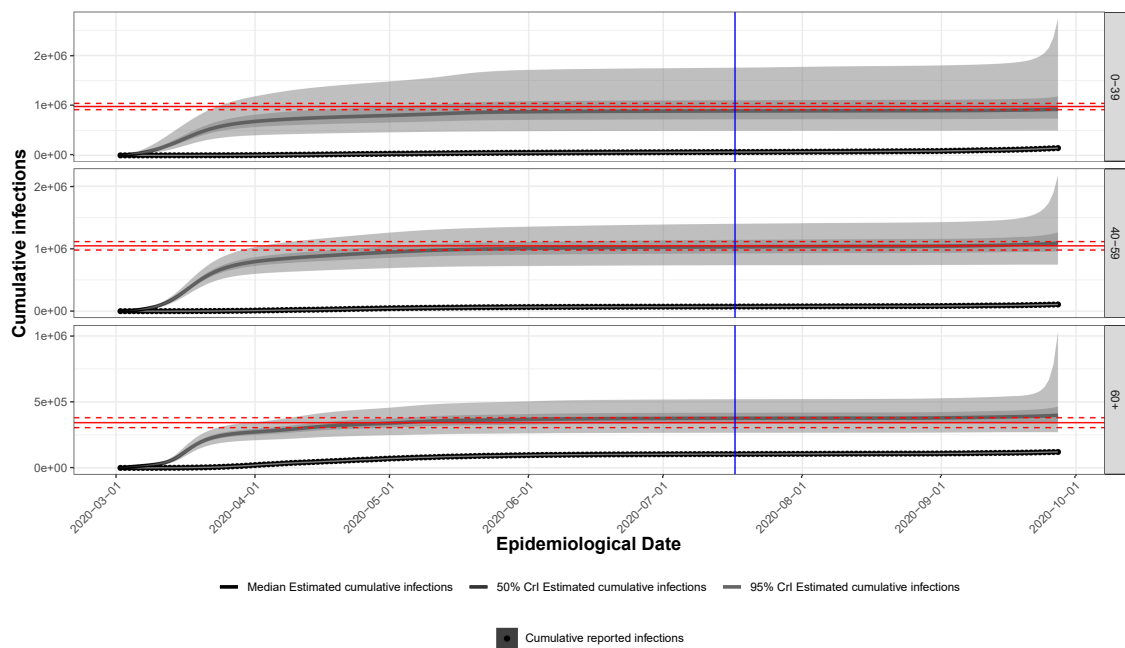


Figure 4: External validation - England. Posterior median age-stratified cumulative infections (50% & 95% credible intervals, CrI) under the MBM model. The age-adjusted estimated counts and the respective 95% confidence intervals of cumulative infections based on REACT-2 (Ward et al., 2021) are represented by the red horizontal lines. The vertical line corresponds to middle of July 2020.